Efficient Small Bandgap Polymer Solar Cells with High Fill Factors for 300 nm Thick Films

*Weiwei Li, Koen H. Hendriks, W. S. Christian Roelofs, Youngju Kim, Martijn M. Wienk, and René A. J. Janssen**

The application of semiconducting conjugated polymers in solution processed polymer solar cells is increasingly successful in terms of achieving high power conversion efficiencies (PCEs) that are now rapidly approaching the 10% milestone.[1] Meanwhile important progress is achieved in roll to roll printing for large-scale fabrication of polymer solar cells.[2] One of the challenges in printing solar cells is the fact that most efficient new materials provide optimal performance for rather thin films (80–120 nm). Although thin (~100 nm) films are generally more efficient they are also more difficult to process reproducibly into pinhole-free large areas at high printing rates. For thick (>200 nm) films this drawback is alleviated and they can absorb more light, but the longer distance over which photogenerated electrons and holes have to be collected increases the bimolecular charge recombination while space charge effects caused by less mobile charges further decrease the fill factor and the PCE.[3] Hence, solution processable materials that provide high efficiencies for thick films are very much in demand. Apart from poly(3-hexylthiophene):[6,6]phenyl-C_{61}-butyric acid methyl ester (P3HT:[60]PCBM) blends,[4] only few studies on conjugated polymers that give a high photovoltaic performance for films above 200 nm have been reported,[5–7] and it is useful to further develop such materials.

Here we present a new diketopyrrolopyrrole-based semiconducting polymer, DT-PDPP-TT (**Figure 1**), that combines a high molecular weight and a small optical bandgap with an absorption up to 920 nm and enables making solar cells with fill factors up to 0.74 with PCEs above 6% for active layers between 100 and 300 nm. The highest PCE of 6.9% is found for a 220 nm thick film. With this excellent performance for thick films we envision that DT-PDPP2T-TT is a useful candidate for printing of organic photovoltaic devices.

The polymer DT-PDPP2T-TT (Figure 1) was designed with diketopyrrolopyrrole (DPP) as a strong electron-deficient unit alternating along the polymer chain with an electron-rich 2,5-di-2-thienylthieno[3,2-*b*]thiophene (2T-TT) segment. Conjugated materials based on DPP units[8–14] and TT units[15–18] have already shown high PCEs in organic solar cells by benefiting from their tendency to crystallize as a result of a rigid conjugated chain with fused aromatic rings.[19,20] Actually, conjugated polymers based on the same PDPP2T-TT motif but different solubilizing side chains such as hexyldecyl (HD-PDPP2T-TT) and octyldodecyl (OD-PDPP2T-TT) have been developed for high performance field-effect transistors (FETs) with electron and hole mobilities exceeding 1 $cm^2\ V^{-1}\ s^{-1}$,[21–24] but so far HD-PDPP2T-TT or OD-PDPP2T-TT gave very modest PCEs (<2%) in solar cells.[25,26] This may be a consequence of the relatively low molecular weight (M_n = 9 kg mol^{-1} for HD[25] and M_n = 22 kg mol^{-1} for OD[26] side chains) and the moderate solubility of the materials. Encouraged by the high charge carrier mobilities, we reasoned that a similar material with longer, decyltetradecyl (DT), side chains would improve the solubility and obtain higher molecular weights in the polymerization reaction. DT-PDPP2T-TT was synthesized via Stille polymerization from 3,6-bis(5-bromo-2-thienyl)-2,5-dihydro-2,5-di(2′-decyltetradecyl)-pyrrolo[3,4c]pyrrolo-1,4-dione and 2,5-bis(trimethylstannyl) thieno[3,2-*b*]thiophene in toluene/DMF (10:1, v/v) using $Pd_2(dba)_3/PPh_3$ as the catalyst system and was purified by Soxhlet extraction, affording a yield of 82%. The molecular weight of the polymer was estimated by gel permeation chromatography (GPC) with *o*-dichlorobenzene (*o*-DCB) as eluent at 80 °C. Under these conditions we measured a very high peak molecular weight of 447 kg mol^{-1} while part of the GPC trace appeared at times earlier than the polystyrene calibration limit molecular weight of 915 kg mol^{-1} (see Supporting Information). The GPC measurements likely represent aggregated polymer chains, but point to a high molecular weight for the new material. High molecular weights are generally beneficial to reach a phase separation and morphology of active layer that provides efficient charge generation and collection for polymer solar cells.[14,27]

The optical absorption spectrum of DT-PDPP2T-TT in chloroform and in thin films exhibits a vibronically structured low energy transition with an onset at about 920 nm (E_g = 1.35 eV) in the solid state (Figure 1b). The spectrum is similar to that of OD-PDPP2T-TT published by Zhang et al.,[26] but is blue-shifted compared to the spectra shown by Li et al.,[21] Chen et al.,[23] and Lee et al.[24] for nominally the same OD-PDPP2T-TT that have onsets close to 1000 nm ($E_g \approx$ 1.2 eV) but show less vibronic fine structure. We found that a low-energy absorption often appears for DPP polymers in which a 3,6-bis(5-bromo-2-thienyl)-2,5-dihydro-2,5-di(alkyl)-pyrrolo[3,4c]pyrrolo-1,4-dione (DPP2T) monomer is used in Stille or Suzuki coupling reactions. We established that the optical bandgap is lowered by adverse homo-coupling reactions of the DPP2T monomers. In our polymerization conditions, such homo-coupling is largely suppressed resulting in a well-defined polymer with blue-shifted

Dr. W. Li, K. H. Hendriks, W. S. C. Roelofs, Y. Kim, Dr. M. M. Wienk, Prof. R. A. J. Janssen
Molecular Materials and Nanosystems
Eindhoven University of Technology
Eindhoven, 5600 MB, The Netherlands
E-mail: r.a.j.janssen@tue.nl

DOI:10. 1002/adma.201300017

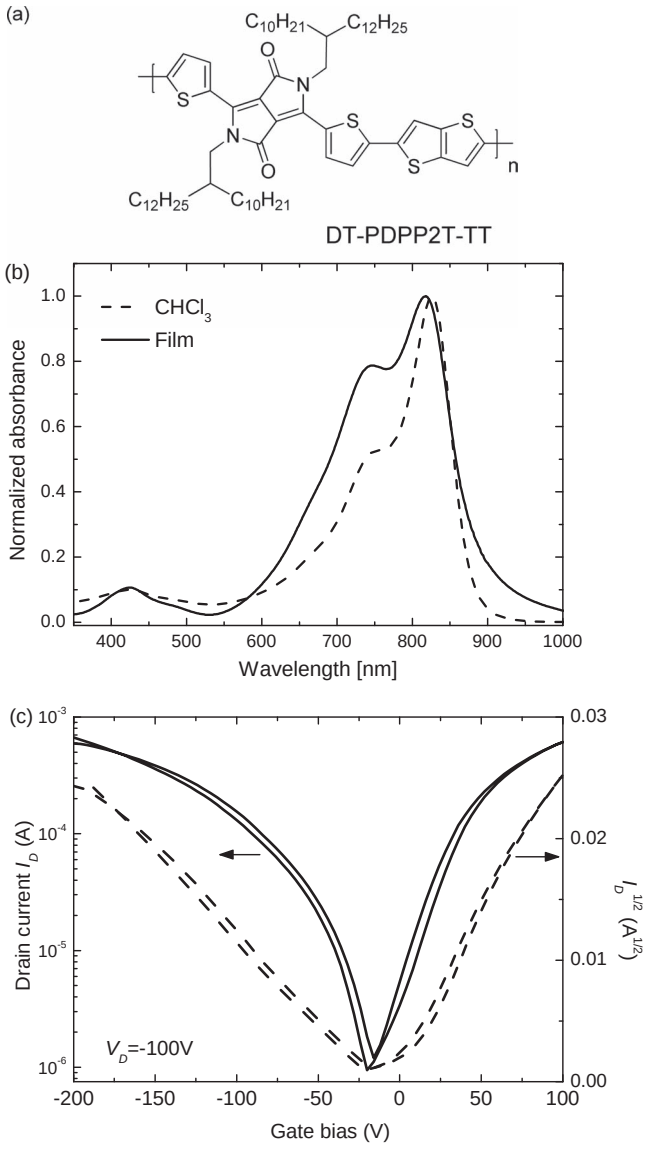

Figure 1. (a) Molecular structure of DT-PDPP2T-TT. (b) Optical absorption spectra of DT-PDPP2T-TT in $CHCl_3$ solution (dashed line) and in solid state films (solid line). (c) Transfer characteristics of a bottom contact–top gate field-effect transistor of DT-PDPP2T-TT, the applied drain bias V_D was –100 V.

and vibronically structured absorption. The HOMO and LUMO levels of DT-PDPP2T-TT have been determined by cyclic voltammetry measurements in *o*-DCB to lie at –0.13 V and –1.55 V vs. Fc/Fc^+, resulting in estimated HOMO and LUMO energy levels of –5.10 and –3.68 eV vs. vacuum. The electrochemical bandgap, E_g^{CV} = 1.42 eV, is slightly higher than the optical bandgap (E_g = 1.35 eV). The charge carrier mobility of DT-PDPP2T-TT has been determined in an FET with a bottom contact–top gate configuration. The FET showed ambipolar behavior with high saturated hole and electron mobilities of 0.8 and 1.5 $cm^2\ V^{-1}\ s^{-1}$, respectively (Figure 1c). We note that the hole mobility of DT-PDPP2T-TT measured here is somewhat higher than the electron mobility of 0.2 $cm^2\ V^{-1}\ s^{-1}$ reported for [60]PCBM in a similar top-contact transistor structure with a polymer dielectric.[28] Although, it is difficult to compare charge carrier mobilities, because these strongly depend on the device configuration, contacts, and measurement conditions, the values indicate that charge transport for holes and electrons in DT-PDPP2T-TT:PCBM blends can be balanced.

DT-PDPP2T-TT was used as electron donor material in bulk heterojunction organic photovoltaic devices with [6,6]phenyl-C_{71}-butyric acid methyl ester ([70]PCBM) as electron acceptor. ITO/PEDOT:PSS and LiF/Al were used as transparent front electrode and reflective back electrode, respectively. The photoactive layers consisting of DT-PDPP2T-TT:[70]PCBM blends were deposited by spin coating. The polymer:fullerene ratio,[29] the nature and composition of the solvent mixture for spin coating, and layer thickness were carefully optimized. The best performing devices were obtained for a 1:3 polymer:fullerene weight ratio spin cast from chloroform containing 7.5 vol.% *o*-DCB. For the optimized devices the PCE is higher than 6% for films with thicknesses between 100 and 300 nm (**Table 1**). The highest performance was obtained for 220 nm thick films and reaches PCE = 6.9%. For this device the short circuit current (J_{sc}) equals 14.8 mA cm^{-2}, the open circuit voltage (V_{oc}) is 0.66 V, and the fill factor (FF) is 0.70 (**Figure 2**a and Table 1). The cell exhibits a broad spectral response. The external quantum efficiency (EQE) reaches 0.63 at 500 nm where [70]PCBM absorbs and 0.35 at 820 nm where DT-PDPP2T-TT absorbs (Figure 2b). The FF of 0.70 for a 220 nm thick photoactive film is presently unsurpassed compared to other small bandgap conjugated polymers. At 300 nm thickness, DT-PDDP2T-TT:[70]PCBM blends still provide FF > 0.60. The good FF indicates efficient charge transport for both electron and holes and evidences that even for such thick active layers bimolecular recombination is limited. We note that the PCE of 6.9% of DT-PDDP2T-TT:[70]PCBM cells is slightly higher than the PCE of 6.7% that was recently reported for a related PDDP3T:[70]PCBM blend.[30]

We analyzed the morphology of the DT-PDDP2T-TT:[70]PCBM blends with AFM and bright-field TEM (**Figure 3**). The surface AFM topology and corresponding phase image give evidence of surface domains that consist of similarly oriented polymers chains or fibers, with lengths of several hundred nanometers.

Table 1. Characteristics of DT-PDPP2T-TT:[70]PCBM solar cells for different layer thickness.

d[n m]	J_{sc}[a)] [mA cm^{-2}]	V_{oc}[V]	FF	PCE [%]
84	11.6	0.68	0.74	5.9
93	12.3	0.68	0.74	6.1
137	12.3	0.67	0.73	6.0
154	13.1	0.66	0.71	6.2
167	12.7	0.66	0.72	6.1
209	14.8	0.66	0.69	6.7
220	14.8	0.66	0.70	6.9
250	15.5	0.67	0.62	6.4
300	15.5	0.67	0.61	6.3
370	15.0	0.66	0.53	5.3

[a)] J_{sc} was calculated by integrating the EQE spectrum with the AM1.5G spectrum.

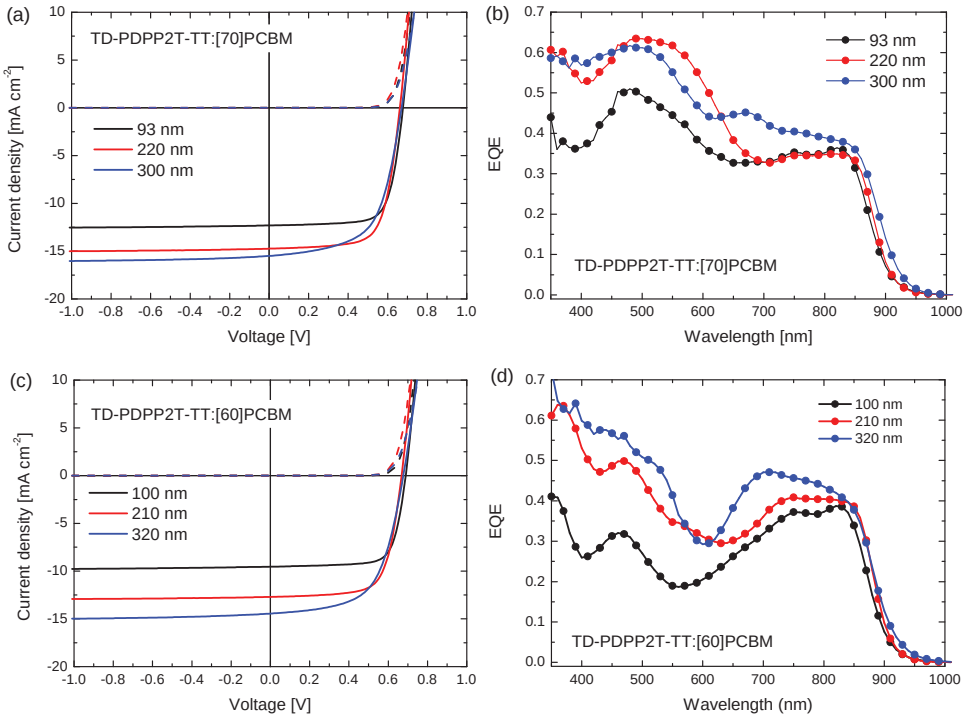

Figure 2. (a, c) *J–V* characteristics in dark (dashed lines) and under white light illumination (solid lines) of optimized solar cells of the polymer DT-PDPP2T-TT with [70]PCBM (a) and [60]PCBM (c) with the different thickness, see legends. (b, d) EQE of the same devices.

The characteristic fibrous surface topology bears similarity to those reported for pure HD- and OD-PDDP2T-TT.[24] The TEM images reveal a complex network structure in the bulk of the film that consists of frequently interconnecting and crossing crystalline fibrous structures with lengths of hundreds and widths of a few tens of nanometers. We conjecture that the high molecular weight of DT- PDPP2T-TT leads to aggregated fibrils in solution that persist in the blend films and enables making sufficient contact with the fullerene acceptor. The fibrous interpenetrating structure of the active layer is beneficial for charge transport.

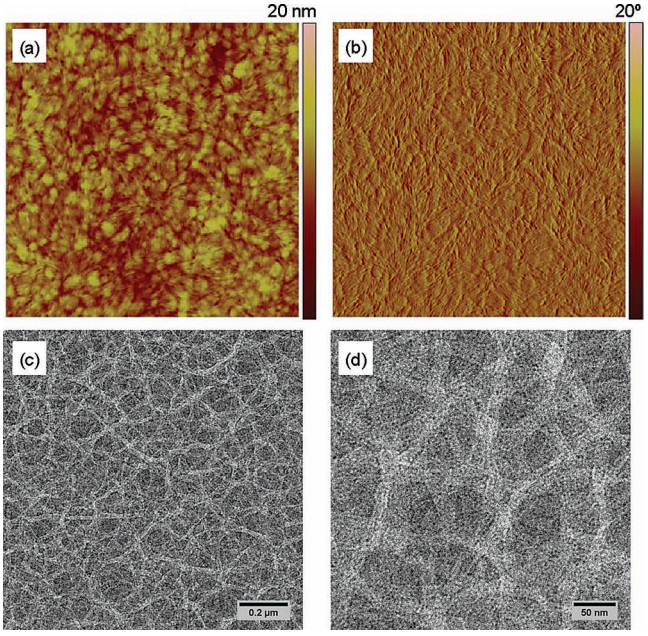

Figure 3. (a) AFM height image of optimized DT-PDPP2T:[70]PCBM surface (3 × 3 µm^2) spin-coated from chloroform containing 7.5 vol.% *o*-DCB. Root mean square (RMS) roughness is 1.75 nm. (b) Corresponding phase image. (c, d) Bright field TEM images (1 × 1 µm^2 and 0.25 × 0.25 µm^2) of the optimized DT-PDPP2T-TT:[70]PCBM blend films. The scale bar in the TEM images is 200 nm (c) and 50 nm (d).

Similarly high photovoltaic performance has been obtained when DT-PDDP2T-TT was mixed with [60]PCBM instead of [70]PCBM (Figure 2c,d, **Table 2**). The best cell had PCE = 6.0%, with J_{sc} = 12.7 mA/cm^2, V_{oc} = 0.67 V, and a FF of 0.71 for a 210 nm thick film. Interestingly, the maximum EQE of 0.40 at 820 nm, where the polymer absorbs, is higher in the blend with [60]PCBM than the value of 0.35 with [70]PCBM. At 500 nm, the value for the blend with [60]PCBM is smaller because of the reduced absorption coefficient of [60]PCBM compared to [70]PCBM. For very thick films the DT-PDDP2T-TT:[60]PCBM (385 nm) cell actually outperforms the DT-PDDP2T-TT:[70]PCBM (370 nm) cell and has a PCE that remains close to 5.8% and FF = 0.60. This would ultimately eliminate the need for using the more expensive [70]PCBM derivative in favor of [60]PCBM.

With these well performing thick photoactive layers, it is of interest to investigate in which conversion steps remaining losses are incurred. We measured the spectral extinction coefficient and refractive index of the two active layers. Using optical modeling that involved the entire stack of layers (glass/ITO/PEDOT:PSS/active layer/LiF/Al) we determined the internal quantum efficiencies (IQE) of the cells by dividing the EQE by the calculated fraction of photons absorbed by the photoactive layer (for details see the Supporting Information). By calculating the total number of AM1.5G photons absorbed in

Table 2. Characteristics of DT-PDPP2T-TT:[60]PCBM solar cells for layer different thickness.

d [nm]	J_{sc}[a)] [mA cm^{-2}]	V_{oc}[V]	FF	PCE [%]
87	8.0	0.69	0.74	4.1
100	9.5	0.69	0.74	4.9
140	10.8	0.68	0.74	5.5
180	11.0	0.67	0.72	5.3
210	12.7	0.67	0.71	6.0
260	12.9	0.68	0.67	5.8
320	14.4	0.68	0.60	5.9
385	14.3	0.67	0.60	5.8

[a)] J_{sc} was calculated by integrating the EQE spectrum with the AM1.5G spectrum.

the photoactive layer and by comparing this to the AM1.5 integrated EQE, it is possible to obtain the spectrally averaged IQE which is plotted for both DT-PDPP2T-TT cells with [60]PCBM and [70]PCBM in **Figure 4** as function of the total layer thickness. The spectrally averaged IQE equals 0.53 ± 0.05 and is identical for layers with either [60]PCBM or [70]PCBM and virtually independent of the layer thickness. This confirms that bimolecular recombination and space charge effects are not limiting the short-circuit current. Nevertheless a significant loss in IQE (0.47 ± 0.05) remains. We attribute this loss to excitons that are lost without generating collectable charges, either via intrinsic decay, quenching at impurity sites, or geminate recombination of charges. It is clear that this represents a significant loss and it is of interest to determine the exact cause.

Tables 1 and 2 show that J_{sc} varies with layer thickness for the DT-PDDP2T-TT:PCBM cells. These differences are mostly due to differences in light absorption because the IQE is essentially constant with layer thickness (Figure 4). For films thicker than 200 nm, also J_{sc} becomes almost constant. In this range, random variations in thickness on different places in one cell will have a minimal effect on the device performance. This provides a processing window for reproducible fabrication of printed solar cells.

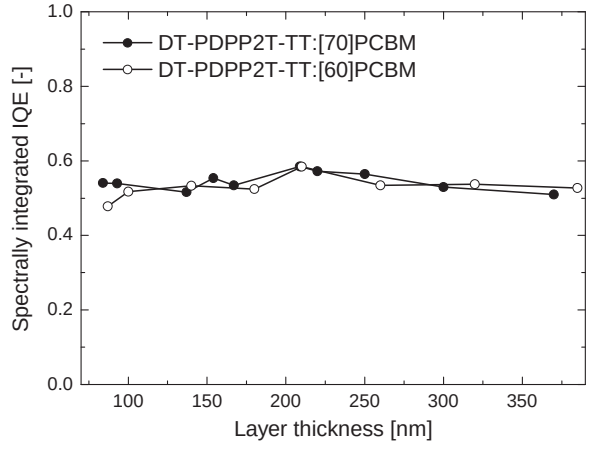

Figure 4. Spectrally averaged IQE for DT-PDPP2T-TT:[70]PCBM and DT-PDPP2T-TT:[60]PCBM solar cells as function of layer thickness.

In conclusion, we have developed a high molecular weight polymer, DT-PDPP2T-TT that has a high hole carrier mobility (0.8 cm^2 V^{-1} s^{-1}) and allows making efficient solar cells for thick (>200 nm) active layers. Blends of DT-PDPP2T-TT with [60]PCBM and [70]PCBM give maximum power conversion efficiencies of 6.0% and 6.9% for films of 210–220 nm thickness. Bimolecular recombination is small as a result of the high charge mobility and a nanomorphology in the film that consists of frequently interconnecting and crossing crystalline fibrous structures with lengths of hundreds and widths of a few tens of nanometers. Achieving high fill factors and efficiencies in organic solar cells with thick films, not only requires donor and acceptor materials with high hole and electron mobilities, but also a morphology that provides efficient percolating pathways for charges together with an essentially field-independent charge separation. The high efficiency for thick layers and its small sensitivity to variations in thickness make DT-PDPP2T-TT:PCBM films a promising candidate for large-scale industry printing applications of polymer solar cells.

Experimental Section

The procedure for synthesizing DT-DPP2T-TT is described in the supporting information. [60]PCBM and [70]PCBM (purity ~95%) were purchased from Solenne BV. Molecular weights were determined with GPC at 80 °C on a PL-GPC 120 system using a PL-GEL 5 µm MIXED-C column and *o*-DCB as the eluent and against polystyrene standards. Electronic spectra were recorded on a Perkin Elmer Lambda 900 UV/vis/nearIR spectrophotometer. Cyclic voltammetry was conducted with a scan rate of 0.1 V s^{-1} under an inert atmosphere with 1 M tetrabutylammonium hexafluorophosphate in *o*-DCB as the electrolyte. The working electrode was a platinum disk, the counter electrode was a silver electrode, and an Ag/AgCl quasi-reference electrode was used. The concentration of the sample in the electrolyte was approximately 1 mM, based on monomers. Fc/Fc$^+$ was used as an internal standard. Tapping mode atomic force microscopy (AFM) was measured on a MFP-3D (asylum research) using PPP-NCHR probes (Nanosensors). TEM was performed on a Tecnai G^2 Sphera TEM (FEI) operated at 200 kV.

Field-effect transistors were prepared in a bottom-contact top-gate configuration on a glass substrate. Source and drain contacts were defined by evaporating gold (30 nm) through a shadow mask. Subsequently the polymer was applied by spin coating from a hot chloroform solution and the residual solvent was dried at 120 °C for 10 min. on a hot plate. The polymer film was further annealed at 200 °C for 10 min. and slowly cooled down to room temperature. Next, a 900 nm PMMA layer was spin coated as gate dielectric and annealed at 120 °C for 30 min. The top gate electrode was applied by evaporating Al (50 nm) through a shadow mask. The transistors were electrically characterized under high vacuum conditions with a Keithley 2636 measuring unit. The length and the width of the transistor channel are 70 µm and 1000 µm, respectively.

Photovoltaic devices were made by spin coating poly-(ethylenedioxythiophene): poly(styrene sulfonate) (PEDOT:PSS) (Clevios P, VP Al 4083) onto pre-cleaned, patterned indium tin oxide (ITO) substrates (14 Ω per square) (Naranjo Substrates). The photoactive layer were deposited by spin coating a chloroform solution containing DT-PDPP2T-TT and [60]PCBM or [70]PCBM with 1:3 (w/w) ratio and the 7.5 vol% of *o*-DCB. LiF (1 nm) and Al (100 nm) were deposited by vacuum evaporation at ~2 × 10^{-7} mbar as the back electrode. The active area of the cells was 0.090 or 0.160 cm^2 and no size dependence was found between these two dimensions. *J–V* characteristics were measured under ~100 mW cm^{-2} white light from a tungsten-halogen lamp filtered by a Schott GG385 UV filter and a Hoya LB 120 daylight filter, using a Keithley 2400 source meter. Short circuit currents under

AM1.5G conditions were estimated from the EQE and integration with the solar spectrum.[21] The current density measured under white light illumination was lower by 9%, with a standard deviation of 2%. The changes in current density with active layer thickness as determined by white light illumination and by integrating the EQE are in very close correspondence.

The EQE was measured under simulated 1 sun operation conditions using bias light from a 532 nm solid state laser (Edmund Optics). Light from a 50 W tungsten halogen lamp (Osram64610) was used as probe light and modulated with a mechanical chopper before passing the monochromator (Oriel, Cornerstone 130) to select the wavelength. The response was recorded as the voltage over a 50 Ω resistance, using a lock-in amplifier (Stanford Research Systems SR 830). A calibrated Si cell was used as reference. The device was kept behind a quartz window in a nitrogen filled container. The thickness of the active layers in the photovoltaic devices was measured on a Veeco Dektak 150 profilometer.

The spectrally internal quantum efficiency (IQE) was determined by optical modeling of the entire layer stack using the wavelength dependent refractive index (n) and extinction coefficient (k).[32] Calculations of the optical electric field were performed with Setfos 3 (Fluxim AG, Switzerland). The spectrally averaged IQE was determined by integrating the EQE of the solar cell with the AM1.5G solar spectrum and dividing by the absorbed photon flux.

Supporting Information

Supporting Information is available from the Wiley Online Library or from the author.

Acknowledgements

We thank Ralf Bovee for GPC analysis and Veronique Gevaerts for TEM measurements. This work was performed in the framework of the "Largecells" project that received funding from the European Commission's Seventh Framework Programme (FP7/2007–2013) under Grant Agreement No. 261936. The research was further supported by the "Europees Fonds voor Regionale Ontwikkeling" (EFRO) in the Interreg IV-A project Organext. The research forms part of the Solliance OPV programme.

Received: January 2, 2013
Published online: March 6, 2013

[1] Z. C. He, C. M. Zhong, S. J. Su, M. Xu, H. B. Wu, Y. Cao, *Nat. Photon.* **2012**, *6*, 591.
[2] R. Sondergaard, M. Hosel, D. Angmo, T. T. Larsen-Olsen, F. C. Krebs, *Mater. Today* **2012**, *15*, 36.
[3] P. W. M. Blom, V. D. Mihailetchi, L. J. A. Koster, D. E. Markov, *Adv. Mater.* **2007**, *19*, 1551.
[4] P. Schilinsky, C. Waldauf, C. J. Brabec, *Appl. Phys. Lett.* **2002**, *81*, 3885.
[5] J. Peet, L. Wen, P. Byrne, S. Rodman, K. Forberich, Y. Shao, N. Drolet, R. Gaudiana, G. Dennler, D. Waller, *Appl. Phys. Lett.* **2011**, *98*, 043301.
[6] T. Y. Chu, J. P. Lu, S. Beaupre, Y. G. Zhang, J. R. Pouliot, S. Wakim, J. Y. Zhou, M. Leclerc, Z. Li, J. F. Ding, Y. Tao, *J. Am. Chem. Soc.* **2011**, *133*, 4250.
[7] S. Lee, S. Nam, H. Kim, Y. Kim, *Appl. Phys. Lett.* **2010**, *97*, 103503.
[8] M. M. Wienk, M. Turbiez, J. Gilot, R. A. J. Janssen, *Adv. Mater.* **2008**, *20*, 2556.
[9] J. C. Bijleveld, A. P. Zoombelt, S. G. J. Mathijssen, M. M. Wienk, M. Turbiez, D. M. de Leeuw, R. A. J. Janssen, *J. Am. Chem. Soc.* **2009**, *131*, 16616.
[10] J. C. Bijleveld, V. S. Gevaerts, D. Di Nuzzo, M. Turbiez, S. G. J. Mathijssen, D. M. de Leeuw, M. M. Wienk, R. A. J. Janssen, *Adv. Mater.* **2010**, *22*, E242.
[11] L. T. Dou, J. B. You, J. Yang, C. C. Chen, Y. J. He, S. Murase, T. Moriarty, K. Emery, G. Li, Y. Yang, *Nat. Photon.* **2012**, *6*, 180.
[12] L. T. Dou, J. Gao, E. Richard, J. B. You, C. C. Chen, K. C. Cha, Y. J. He, G. Li, Y. Yang, *J. Am. Chem. Soc.* **2012**, *134*, 10071.
[13] A. T. Yiu, P. M. Beaujuge, O. P. Lee, C. H. Woo, M. F. Toney, J. M. J. Fréchet, *J. Am. Chem. Soc.* **2012**, *134*, 2180.
[14] W. Li, W. S. C. Roelofs, M. M. Wienk, R. A. J. Janssen, *J. Am. Chem. Soc.* **2012**, *134*, 13787.
[15] Y. N. Li, P. Sonar, S. P. Singh, Z. E. Ooi, E. S. H. Lek, M. Q. Y. Loh, *Phys. Chem. Chem. Phys.* **2012**, *14*, 7162.
[16] H. Bronstein, Z. Chen, R. S. Ashraf, W. Zhang, J. Du, J. R. Durrant, P. S. Tuladhar, K. Song, S. E. Watkins, Y. Geerts, M. M. Wienk, R. A. J. Janssen, T. Anthopoulos, H. Sirringhaus, M. Heeney, I. McCulloch, *J. Am. Chem. Soc.* **2011**, *133*, 3272.
[17] G. Y. Chen, Y. H. Cheng, Y. J. Chou, M. S. Su, C. M. Chen, K. H. Wei, *Chem. Commun.* **2011**, *47*, 5064.
[18] X. Guo, M. J. Zhang, L. J. Hou, C. H. Cui, Y. Wu, J. H. Hou, Y. Li, *Macromolecules* **2012**, *45*, 6930.
[19] C. B. Nielsen, M. Turbiez, I. McCulloch, *Adv. Mater.* **2012**, DOI: 10.1002/adma.201201795.
[20] I. McCulloch, M. Heeney, C. Bailey, K. I, M. Genevicius, M. Shkunov, D. Sparrowe, S. Tierney, R. Wagner, W. M. Zhang, M. L. Chabinyc, R. J. Kline, M. D. McGehee, M. F. Toney, *Nat. Mater.* **2006**, *5*, 328.
[21] Y. Li, S. P. Singh, P. Sonar, *Adv. Mater.* **2010**, *43*, 4862.
[22] X. Zhang, L. J. Richter, D. M. DeLongchamp, R. J. Kline, M. R. Hammond, I. McCulloch, M. Heeney, R. S. Ashraf, J. N. Smith, T. D. Anthopoulos, B. Schroeder, Y. H. Geerts, D. A. Fischer, M. F. Toney, *J. Am. Chem. Soc.* **2011**, *133*, 15073.
[23] Z. Y. Chen, M. J. Lee, R. S. Ashraf, Y. Gu, S. Albert-Seifried, M. M. Nielsen, B. Schroeder, T. D. Anthopoulos, M. Heeney, I. McCulloch, H. Sirringhaus, *Adv. Mater.* **2012**, *24*, 647.
[24] J. S. Lee, S. K. Son, S. Song, H. Kim, D. R. Lee, K. Kim, M. J. Ko, D. H. Choi, B. Kim, J. H. Cho, *Chem. Mater.* **2012**, *24*, 1316.
[25] J. C. Bijleveld, R. A. M. Verstrijden, M. M. Wienk, R. A. J. Janssen, *J. Mater. Chem.* **2011**, *21*, 9224.
[26] G. B. Zhang, Y. Y. Fu, Z. Y. Xie, Q. Zhang, *Sol. Energy Mater. Sol. Cells* **2011**, *95*, 1168.
[27] R. C. Coffin, J. Peet, J. Rogers, G. C. Bazan, *Nat. Chem.* **2009**, *1*, 657.
[28] T. B. Singh, N. Marjanovic, P. Stadler, M. Auinger, G. J. Matt, S. Günes, N. S. Sariciftci, R. Schwödiauer, S. Bauer, *J. Appl. Phys.* **2005**, *97*, 083714.
[29] X. Guo, M. Zhang, J. Tan, S. Zhang, L. Huo, W. Hu, Y. Li, J. Hou, *Adv. Mater.* **2012**, *24*, 6536.
[30] L. Ye, S. Zhang, W. Ma, B. Fan, X. Guo, Y. Huang, H. Ade, J. Hou, *Adv. Mater.* **2012**, *24*, 6335.
[31] D. J. Wehenkel, K. H. Hendriks, M. M. Wienk, R. A. J. Janssen, *Org. Electron.* **2012**, *13*, 3284.
[32] J. Gilot, M. M. Wienk, R. A. J. Janssen, *Adv. Mater.* **2010**, *22*, E67.